Compiled records of carbon isotopes in atmospheric CO_2 for historical simulations in CMIP6

Heather Graven[1], Colin E. Allison[2], David M. Etheridge[2], Samuel Hammer[3], Ralph F. Keeling[4], Ingeborg Levin[3], Harro A. J. Meijer[6], Mauro Rubino[5], Pieter P. Tans[7], Cathy M. Trudinger[2], Bruce H. Vaughn[8], James W. C. White[8]

[1]Department of Physics, Imperial College London, UK
[2]CSIRO Climate Science Centre, Oceans and Atmosphere, Aspendale, Australia
[3]Institut für Umweltphysik, Heidelberg University, Germany
[4]Scripps Institution of Oceanography, University of California, San Diego, USA
[5]Dipartimento di Matematica e Fisica, Università della Campania "Luigi Vanvitelli", Caserta, Italy
[6]Centre for Isotope Research, University of Groningen, The Netherlands
[7]National Oceanic and Atmospheric Administration, Boulder, USA
[8]Institute of Arctic and Alpine Research, University of Colorado, Boulder, USA

Correspondence to: Heather Graven (h.graven@imperial.ac.uk)

Abstract. The isotopic composition of carbon ($\Delta^{14}C$ and $\delta^{13}C$) in atmospheric CO_2 and in oceanic and terrestrial carbon reservoirs is influenced by anthropogenic emissions and by natural carbon exchanges, which can respond to and drive changes in climate. Simulations of ^{14}C and ^{13}C in the ocean and terrestrial components of Earth System Models (ESMs) present opportunities for model evaluation and for investigation of carbon cycling, including anthropogenic CO_2 emissions and uptake. The use of carbon isotopes in novel evaluation of the ESMs' component ocean and terrestrial biosphere models and in new analyses of historical changes may improve predictions of future changes in the carbon cycle and climate system. We compile existing data to produce records of $\Delta^{14}C$ and $\delta^{13}C$ in atmospheric CO_2 for the historical period 1850-2015. The primary motivation for this compilation is to provide the atmospheric boundary condition for historical simulations in the Coupled Model Intercomparison Project 6 (CMIP6) for models simulating carbon isotopes in the ocean or terrestrial biosphere. The data may also be useful for other carbon cycle modelling activities.

1 Introduction

The isotopic composition of carbon in atmospheric, ocean and terrestrial reservoirs has been strongly perturbed by human activities since the Industrial Revolution. Fossil fuel burning is diluting the proportion of the isotopes ^{14}C and ^{13}C relative to ^{12}C in atmospheric CO_2 by the addition of aged, plant-derived carbon that is partly depleted in ^{13}C and entirely depleted in ^{14}C. This process is referred to as the Suess Effect following the early observations of radiocarbon in tree rings by Hans Suess (Suess, 1955; Revelle and Suess, 1957). The term Suess Effect was also later adopted for ^{13}C (Keeling, 1979). The magnitudes of the atmospheric ^{14}C and ^{13}C Suess Effects are determined not only by fossil fuel emissions, but also by carbon exchanges with the ocean and terrestrial reservoirs and the residence time of carbon in these reservoirs, which regulate the mixing of the fossil fuel signal out of the atmosphere (Stuiver and Quay, 1981; Keeling, 1979). In addition, some biological and physical processes cause isotopic fractionation and the associated fractionation factors can vary with environmental conditions. Land use changes can also influence carbon isotope composition (Scholze et al., 2008). Variations in ^{13}C are reported as $\delta^{13}C$, which represents deviations in $^{13}C/^{12}C$ from a standard reference

material (VPDB). For ^{14}C, the notation $\Delta^{14}C$ is used, which represents deviations from the Modern standard $^{14}C/C$ ratio and includes a correction for mass-dependent isotopic fractionation based on $\delta^{13}C$ as well as a correction for ^{14}C radioactive decay of the sample (Stuiver and Polach, 1977).

In addition to the perturbation from fossil fuel emissions, atmospheric $\Delta^{14}C$ was also subject to a large, abrupt perturbation in the 1950s and 60s when a large amount of ^{14}C was produced during atmospheric nuclear weapons testing. The introduction of this "bomb ^{14}C" nearly doubled the amount of ^{14}C in the Northern Hemisphere troposphere, where most of the tests took place (Rafter and Fergusson, 1957; Münnich and Vogel, 1958). Most testing stopped after 1962 due to the Partial Test Ban Treaty, after which tropospheric $\Delta^{14}C$ decreased quasi-exponentially as bomb ^{14}C mixed through the atmosphere and into carbon reservoirs in the ocean and terrestrial biosphere that exchange with the atmosphere on annual to decadal timescales (Levin and Hesshaimer, 2000).

Sustained, direct atmospheric measurements of $\Delta^{14}C$ in CO_2 began in 1955 in Wellington, New Zealand, capturing the dramatic changes over the weapons testing period (Rafter and Fergusson, 1957; Manning et al., 1990; Currie et al., 2009). Observations of $\Delta^{14}C$ at several more stations started in the late 1950s, with some ceasing operation by the 1970s (Nydal and Lövseth, 1983; Levin et al., 1985). For $\delta^{13}C$ in CO_2, sustained flask sampling programs began in 1977-78 at the South Pole (Antarctica), Christmas Island, and La Jolla and Mauna Loa (USA) (Keeling et al., 1979; Keeling et al., 2001), and in 1978 at Cape Grim (Australia) (Francey and Goodman, 1986; Francey et al., 1996). A global network for $\Delta^{14}C$ measurements is currently run by Heidelberg University (Levin et al., 2010), while global networks for $\delta^{13}C$ measurements are run by Scripps Institution of Oceanography (SIO) (Keeling et al., 2005), the Commonwealth Scientific and Industrial Research Organisation (CSIRO) (Allison and Francey, 2007), and jointly by the University of Colorado Institute for Arctic and Alpine Research and the National Oceanic and Atmospheric Administration (referred to here as NOAA) (Vaughn et al., 2010). Several other groups are also conducting long-term isotopic CO_2 observations at individual sites or in regional networks.

Records of atmospheric $\Delta^{14}C$ and $\delta^{13}C$ have been extended into the past using measurements of tree rings and of CO_2 in air from ice sheets (ice cores and firn) respectively; recent examples include Reimer et al. (2013) and Rubino et al. (2013). Ice cores are generally not used to construct atmospheric $\Delta^{14}C$ records due to in situ ^{14}C production, and tree rings are generally not used to construct atmospheric $\delta^{13}C$ records due to climatic and physiological influences on ^{13}C discrimination. These records clearly show decreases in $\Delta^{14}C$ and $\delta^{13}C$ due to increased emissions of fossil-derived carbon following the Industrial Revolution and carbon from land use change. Ice cores, and tree ring and other proxy records (e.g. lake macrofossil, marine foraminifera, coral and speleothem records) additionally reveal decadal to millennial variations associated with climate and carbon cycle variability, and, for ^{14}C, changes in solar activity and the geomagnetic field (Damon et al., 1978).

Studies using $\Delta^{14}C$ and $\delta^{13}C$ observations of carbon in the atmosphere, ocean and terrestrial biosphere together with simulated ^{14}C and ^{13}C dynamics in models can provide insights to key processes in the global carbon cycle including air-sea gas exchange, ocean mixing, water use efficiency in plants, and vegetation and soil carbon turnover rates. Ocean $\Delta^{14}C$ observations have been separated into "natural" and "bomb" ^{14}C components (Key et al., 2004) and combined with models to constrain the global air-sea gas exchange velocity (Naegler, 2009;

Sweeney et al., 2007), and to constrain or identify biases in ocean model transport and mixing (Oeschger et al., 1975; Matsumoto et al., 2004; Khatiwala et al., 2009). Observations of $\delta^{13}C$ in ocean dissolved inorganic carbon have been used to investigate anthropogenic CO_2 uptake (Quay et al., 2003) and to evaluate ocean models that include marine ecosystem dynamics (Tagliabue and Bopp, 2008; Schmittner et al., 2013). With terrestrial biosphere models, simulations of the response of plants and photosynthesis to rising atmospheric CO_2 and changing water availability can be evaluated with $\delta^{13}C$ observations in atmospheric CO_2 or in leaves or tree rings, because a close relationship exists between processes controlling leaf-level isotopic discrimination and water-use efficiency (Randerson et al., 2002; Scholze et al., 2008; Ballantyne et al., 2011; Keller et al., 2017; Keeling et al., 2017). Additionally, observations of $\Delta^{14}C$ can be used to constrain models of carbon turnover rates in vegetation and soil carbon at plot-level and global scales (Trumbore, 2000; Naegler and Levin, 2009).

The Coupled Model Intercomparison Project phase 6 (CMIP6, Eyring et al., 2016) is leading the coordination of current global earth system modelling activities. CMIP6 follows the previous phase CMIP5 that contributed to the Intergovernmental Panel on Climate Change's Fifth Assessment Report (IPCC, 2013). CMIP6 is organizing common standards for reporting of model output and protocols for a set of core experiments including historical simulations and for several additional specialized experiments. The specialized experiments focus on individual processes or time periods and they are referred to as CMIP6-endorsed MIPs, which are organized by separate committees. Ocean MIP (OMIP) focuses on historical ocean physics and biogeochemistry and provides a separate set of simulation protocols including climatic forcing provided by atmospheric reanalyses (Griffies et al., 2016; Orr et al., 2017). The Coupled Climate–Carbon Cycle MIP (C4MIP) encompasses historical, future, and idealized biogeochemical simulations in both the ocean and the terrestrial biosphere, using climatic forcing from coupled ESMs as opposed to observations (Jones et al., 2016). For any historical simulations in CMIP6 that use observed atmospheric greenhouse gas concentrations to drive the Earth system models, compiled records of atmospheric CO_2 and other greenhouse gas concentrations are provided by Meinshausen et al. (2017). Here we describe a compilation of historical data for carbon isotopes in atmospheric CO_2 to support the inclusion of carbon isotope modelling in CMIP6. The carbon isotope datasets are provided in Table S1 and available at input4MIPs (Graven et al. 2017ab): https://esgf-node.llnl.gov/search/input4mips/.

By providing atmospheric datasets for $\Delta^{14}C$ and $\delta^{13}C$ in CO_2 as part of CMIP6, we hope to stimulate more activity in carbon isotope modelling. So far, the inclusion of carbon isotopes in large-scale models and model intercomparisons has been limited. Carbon isotopes were not included in CMIP5, the previous phase of coupled model intercomparison. One study, the Ocean Carbon Cycle Model Intercomparison Project 2 (OCMIP2), used simulations of ocean ^{14}C to evaluate modelled ocean circulation and its effects on simulated anthropogenic CO_2 uptake and marine biogeochemistry (Orr et al., 2001; Matsumoto et al., 2004). Model intercomparisons for ^{13}C in the ocean, and for both ^{13}C and ^{14}C in the terrestrial biosphere have not been performed. This may be partly a result of the small number of carbon cycle models presently simulating carbon isotopes, although some simulations with global models that don't explicitly include carbon isotopes have been possible by using off-line isotope models (Joos et al., 1996; Thompson and Randerson, 1999; Graven et al., 2012a; He et al., 2016).

In this paper, we first review how carbon isotopes are being included in the protocols for CMIP6, which are described in more detail in Orr et al. (2017) and Jones et al. (2016). We then describe the historical atmospheric

datasets we compiled for $\delta^{13}C$ and $\Delta^{14}C$ in CO_2. We refer to the compiled datasets as "forcing datasets" to emphasize that (i) they are intended for model input data, (ii) atmospheric observations have been used to calculate annual and spatial averages, and (iii) some observations have been adjusted as described below. Because of these modifications, the forcing data are not intended to be used in atmospheric inversions. For that purpose we direct modellers to the original atmospheric observations used to produce the forcing datasets, available through data repositories listed in Table 1. The firn and ice core data, updated from Rubino et al. (2013), are available in Table S2.

2 Historical Simulations of Carbon Isotopes in CMIP6

For CMIP6, carbon isotopes are included in historical biogeochemical simulations as part of OMIP (Ocean MIP (Orr et al., 2017)) and C4MIP (Coupled Climate–Carbon Cycle MIP (Jones et al., 2016)). Carbon isotopes will also be included in the simulation of future scenarios. In a separate paper, we will provide atmospheric $\Delta^{14}C$ and $\delta^{13}C$ for future scenarios in CMIP6 created with a simple carbon cycle model (Graven, 2015) and CO_2 emission and concentration scenarios from ScenarioMIP (O'Neill et al., 2016).

The CMIP6 simulation protocols for carbon isotopes are provided in detail in Orr et al. (2017) and Jones et al. (2016), so only a short summary is given here. The variables requested for CMIP6 are stocks and fluxes of ^{14}C and ^{13}C from any model including ^{14}C or ^{13}C in the land or ocean component. Stocks and fluxes of ^{14}C should be reported with a normalization factor of 1/Rs where Rs is the standard $^{14}C/C$ ratio, 1.176×10^{-12} (Karlen et al., 1965) whereas ^{13}C should be reported without normalization. For the ocean, the variables requested are the net air-sea fluxes of ^{14}C and ^{13}C and the dissolved inorganic ^{14}C and ^{13}C concentration (Jones et al., 2016; Orr et al., 2017). Models simulating dissolved inorganic ^{13}C concentration typically include ^{13}C in their marine ecosystem model (Tagliabue and Bopp, 2008; Schmittner et al., 2013) because the oceanic $\delta^{13}C$ distribution is strongly affected by marine productivity and organic matter remineralization. Models can simulate ^{14}C as an abiotic variable with corresponding abiotic carbonate chemistry (Orr et al., 2017) because the oceanic $\Delta^{14}C$ distribution is largely insensitive to biological activity (Fiadeiro, 1982), although some models might also include ^{14}C in their marine ecosystem model (Jahn et al., 2015). For the terrestrial biosphere, ^{14}C and ^{13}C fluxes associated with gross primary productivity, autotrophic respiration and heterotrophic respiration are requested. Stocks of ^{14}C and ^{13}C in vegetation, litter and soil should also be reported.

Expected uses for historical carbon isotope simulations in CMIP6 include the evaluation of modelled ocean CO_2 uptake and transport and carbon cycling in marine ecosystems, the evaluation of modelled carbon fluxes and stocks in terrestrial ecosystems and the ecosystem responses to higher CO_2 and ecohydrological changes, and the interpretation of atmospheric data. Including carbon isotopes in CMIP6 may also prepare for and motivate more activity in carbon isotope modelling in future work.

3 Historical atmospheric forcing dataset for $\Delta^{14}C$ in CO_2

We compiled historical data for $\Delta^{14}C$ in CO_2 from tree ring records and atmospheric measurements to produce the historical atmospheric forcing dataset. We use the data to estimate annual mean values for three zonal bands representing the Northern Hemisphere (north of 30°N), the Tropics (30°S-30°N) and the Southern Hemisphere

(south of 30°S), shown in Figure 1. Here we describe the datasets used in the compilation, and a summary of datasets used in different time periods is given in Table S3.

For 1850-1940, we use estimates of $\Delta^{14}C$ in CO_2 from previous compilations of tree rings and other records that define the calibration curves used for radiocarbon dating. Separate estimates have been made for the Northern Hemisphere, IntCal13 (Reimer et al., 2013), and for the Southern Hemisphere, SHCal13 (Hogg et al., 2013). Linear interpolation was used to estimate annual values from data with 5-year resolution provided by IntCal13 and SHCal13. We estimate $\Delta^{14}C$ in the Tropics as the average of the Northern and Southern Hemispheres for 1850-1940. This estimate is consistent with annual tree ring measurements from 22°S in Brazil over 1927-1940 (Santos et al., 2015), which are 2.2 ± 2.5 ‰ lower than the average of Northern and Southern Hemisphere $\Delta^{14}C$. We did not find tropical tree ring data available for the period 1850-1927, but measurements from northern Thailand in an earlier period 1600-1800 were bracketed by measurements from New Zealand and USA (Hua et al., 2004), suggesting the average of Northern and Southern Hemisphere $\Delta^{14}C$ is likely to provide a reasonable estimate of tropical $\Delta^{14}C$.

For the period between 1940 and 1954, we set $\Delta^{14}C$ in the Southern Hemisphere and Tropics to be the same as the Northern Hemisphere $\Delta^{14}C$, where Northern Hemisphere $\Delta^{14}C$ is given by IntCal13 over 1940-50 and by tree ring data from Stuiver and Quay (1981) over 1951-54. We therefore fix the spatial $\Delta^{14}C$ gradients at 0 ‰ over this period 1940-55. This approach is motivated by differences between the Southern Hemisphere $\Delta^{14}C$ in 1950 in SHCal13 and another compilation of tree ring data by Hua et al. (2013). In SHCal13, Southern Hemisphere $\Delta^{14}C$ becomes 4 ‰ higher than Northern Hemisphere $\Delta^{14}C$ over 1940-50, after being similar to Northern Hemisphere $\Delta^{14}C$ over 1915-40. However in Hua et al. (2013), Southern Hemisphere $\Delta^{14}C$ is only 1 ‰ higher than Northern Hemisphere $\Delta^{14}C$, north of 40°N, in 1950. Tree ring measurements from Brazil in 1940-1954 (Santos et al., 2015) are also consistent with Northern Hemisphere $\Delta^{14}C$, with an average difference of -0.5 ± 1.9 ‰ for the tree ring data minus Northern Hemisphere $\Delta^{14}C$ in IntCal13. There is no significant difference between Northern Hemisphere $\Delta^{14}C$ in IntCal13 and Hua et al. (2013) in 1950.

For Southern Hemisphere $\Delta^{14}C$ over 1955-2015, we use direct measurements of atmospheric $\Delta^{14}C$, primarily the measurements conducted by Heidelberg University (Levin et al., 2010, Levin et al. unpublished). However, we use data from 1955 through 1983 made by the Rafter Radiocarbon Laboratory at Wellington, New Zealand, to specify $\Delta^{14}C$ in the Southern Hemisphere for 1955-83. A correction of -4 ‰ is added to the Wellington data, as reported in Manning and Melhuish (1994), to account for a systematic difference between the Wellington and Heidelberg laboratories. For 1984-2014, data from Heidelberg University (Levin et al., 2010) from Neumayer (Antarctica), Cape Grim (Australia) and Macquarie Island (Australia) are averaged, if available, and where there is missing data the following procedure is used. If Macquarie Island data are missing, averages from Neumayer and Cape Grim are adjusted by -1.2‰, the average difference in mean $\Delta^{14}C$ across the three sites when available Macquarie Island data are included or not. This adjustment takes into account that $\Delta^{14}C$ observed at Macquarie Island is lower than the stations further north and south, resulting from gas exchange over the Southern Ocean (Levin and Hesshaimer, 2000). Macquarie Island data are available for 1993-1999, 2003, 2007-09 and 2011. For 2015, only Neumayer data were available, so the annual mean at Neumayer was adjusted by -2‰, which is the mean difference between Neumayer and the calculated Southern Hemisphere average for 2010-14.

For the Northern Hemisphere, $\Delta^{14}C$ for 1955 to 1958 is based on tropospheric data compiled by Tans (1981). From 1959-1984, $\Delta^{14}C$ observations from Vermunt, Austria are used (Levin et al., 1985). For the years 1985-86, only a few observations from Vermunt are available. Observations by Heidelberg University from Izaña began in 1984 and from Jungfraujoch, Switzerland in 1986. Sampling at Alert, Canada started in 1989. Even though Izaña is located at 28°N, slightly south of the 30°N bound, we use data from Izaña to specify Northern Hemisphere $\Delta^{14}C$ for the period 1985-88 when very little data are available, after correcting for the mean difference between Izaña and the average of Izaña, Jungfraujoch, and Alert over 1989-97. For 1989-97, the average of Izaña, Jungfraujoch, and Alert is used. For 1997-2010, the average of Jungfraujoch, Alert and Mace Head, Ireland is used. From 2011-2015, only Jungfraujoch data are available (Hammer and Levin, 2017), which were used here but adjusted by +0.4‰, taking into account that Jungfraujoch is influenced slightly more by fossil fuel CO_2 than Alert and Mace Head further north (see also Levin and Hesshaimer, 2000).

Observations in the tropics were made by the Heidelberg laboratory for the period 1991-97 at Mérida, Venezuela (8°N), and the annual averages at Mérida are used to specify tropical $\Delta^{14}C$ for 1991-97. Measurements at Mérida were 2.9 ‰ higher than the Northern Hemisphere $\Delta^{14}C$ over 1991-97, on average, and the difference (2.9 ‰) was applied to Northern Hemisphere $\Delta^{14}C$ to estimate tropical $\Delta^{14}C$ for the periods 1985-1991 and 1998-2015. To estimate tropical $\Delta^{14}C$ before 1985, an atmospheric box model was used together with Northern and Southern Hemisphere $\Delta^{14}C$ data. The atmospheric box model is part of a carbon cycle model which also simulates other atmospheric species and radioisotopes, and the model exchange parameters were optimized to match atmospheric data including $\Delta^{14}C$, SF_6 and $^{10}Be/^{7}Be$ (Naegler and Levin, 2006). The model includes six tropospheric boxes separated at the Equator and 30° and 60° in each hemisphere. For each hemisphere, we calculated the ratio between simulated annual $\Delta^{14}C$ averaged in the tropical boxes and simulated annual $\Delta^{14}C$ averaged in the polar boxes. The annual average tropical-to-polar ratio was then multiplied by the observed average Northern and Southern Hemisphere $\Delta^{14}C$ for each year to yield the values for the tropics before 1985.

A preliminary version of the $\Delta^{14}C$ data compilation (version 1.0) was released in early 2017 via email to C4MIP and OMIP researchers and at input4MIPs (https://esgf-node.llnl.gov/search/input4mips/). The version we describe here (version 2.0, Graven et al. 2017b) incorporates new and updated $\Delta^{14}C$ data from Heidelberg University (Hammer and Levin, 2017; Levin et al. unpublished data), whereas version 1.0 was based on fewer data and on extrapolated values for the last few years. For the Northern Hemisphere, $\Delta^{14}C$ for 2011-15 was updated in version 2.0 but $\Delta^{14}C$ for 2010 and earlier is the same as in version 1. For the Southern Hemisphere, $\Delta^{14}C$ for 2000-2015 was updated. For the tropics, $\Delta^{14}C$ for 1998-2015 was updated. Differences between version 1.0 and version 2.0 are smaller than 3.5 ‰ for individual years, and average -0.2 ‰ for the Northern Hemisphere (2011-2015), 0.0 ‰ for the tropics (1998-2015) and -1.3 ‰ for the Southern Hemisphere (2000-2015). Both versions are available at input4MIPs.

Here we make some comparisons with other reported atmospheric $\Delta^{14}CO_2$ measurements. Organized comparisons between laboratories conducting atmospheric $\Delta^{14}CO_2$ measurements using reference air were initiated around 2005, and results to date indicate that most laboratories are currently compatible within 2-3 ‰ (Miller et al., 2013; Hammer et al., 2016), which is similar to current measurement uncertainty but not within

the current goal of <1‰ from the World Meteorological Organization (WMO/IAEA, 2016). Whereas the compilation we report here primarily uses the measurements of the global network of Heidelberg University, continued efforts to compare $\Delta^{14}C$ measurements from different laboratories could help to incorporate more laboratories in future data compilations.

In comparisons of the Southern Hemisphere $\Delta^{14}C$ forcing data with observations at the South Pole, differences are less than 2 ‰ with data from SIO and Lawrence Livermore National Laboratory (LLNL) over 2000-07 and differences are approx. 5 ‰ with University of Groningen data from 1987-89 (Meijer et al., 2006; Graven et al., 2012c). Observations from Wellington, New Zealand from 1983 to 2014 also show similar trends (Turnbull et al., 2016). Differences are less than 3.5 ‰ in comparisons of the Northern Hemisphere $\Delta^{14}C$ forcing data with annual mean $\Delta^{14}C$ from SIO/LLNL observations at Point Barrow and La Jolla for 2002-07, and with University of Groningen observations at Point Barrow for 1987-89. The Northern Hemisphere $\Delta^{14}C$ forcing data also compares well with observations at Niwot Ridge, Colorado, where trends of -4 to -6 ‰ yr^{-1} have been observed since 2004 (Turnbull et al., 2007; Lehman et al., 2016). Estimated tropical $\Delta^{14}C$ shows good agreement with observations of $\Delta^{14}C$ at Hawaii and Samoa for 2002-07 made by SIO/LLNL (Graven et al., 2012c), with differences less than 1.5 ‰ compared to the annual averages of Mauna Loa, Kumukahi and Samoa. A limited amount of data available for Mauna Loa, Kumukahi and Samoa from 2014-15 is also consistent with the estimated tropical $\Delta^{14}C$. Our estimate for tropical $\Delta^{14}C$ in the 1960s lies between observations from Ethiopia and Madagascar made at the Trondheim laboratory (Nydal and Lövseth, 1983). The Trondheim data were not used directly since no comparison between Heidelberg University and the Trondheim laboratory took place, however future studies could potentially incorporate the Trondheim data, which are available at the Carbon Dioxide Information Analysis Center (see Table 1).

A comparison with the data compilation covering 1950-2010 including tree ring and atmospheric $\Delta^{14}C$ data by Hua et al. (2013) is shown in Fig. 2. The range in tree ring $\Delta^{14}C$ data overlaps the Northern and Southern Hemisphere $\Delta^{14}C$ forcing data in all periods, showing good consistency between the records. Hua et al. (2013) separate data from tropical regions over the period 1950-1972, which also overlap the CMIP6 tropical $\Delta^{14}C$ forcing data for 1950-1972 (not shown in Fig. 2).

The data compilation shows the trends and spatial gradients in $\Delta^{14}C$ of CO_2 over the historical period since 1850, as reported in previous studies. Between 1850 and 1952, atmospheric $\Delta^{14}C$ decreased from approximately -4 ‰ to a minimum value around -25 ‰ as emissions from fossil fuel combustion increased after the Industrial Revolution. In the preindustrial and early industrial period to 1915, $\Delta^{14}C$ was 3-6 ‰ lower in the Southern Hemisphere than the Northern Hemisphere due to the negative influence of CO_2 exchange with aged, ^{14}C-depleted waters upwelling in the Southern Ocean (Braziunas et al., 1995; Rodgers et al., 2011; Lerman et al., 1970; Levin et al., 1987). Between 1915 and 1955, the interhemispheric gradient decreased due to the growth in fossil fuel emissions, which are concentrated in the Northern Hemisphere (McCormac et al., 1998). After 1955, $\Delta^{14}C$ increased rapidly as a result of nuclear weapons testing, reaching a maximum of 836 ‰ in the Northern Hemisphere and 637 ‰ in the Southern Hemisphere, where the values 836 ‰ and 637 ‰ are the maxima in the forcing data. $\Delta^{14}C$ was even higher in the stratosphere and some Northern Hemisphere sites (Hesshaimer and Levin, 2000). After 1963-64, tropospheric $\Delta^{14}C$ decreased quasi-exponentially as the bomb ^{14}C mixed with

oceanic and biospheric carbon reservoirs while growing fossil fuel emissions continued to dilute atmospheric $^{14}CO_2$. Differences between the Northern and Southern Hemisphere reduced rapidly and were close to zero for the 1980s-90s (Meijer et al., 2006; Levin et al., 2010; Levin and Hesshaimer, 2000), until the mid-2000s when a Northern deficit in $\Delta^{14}C$ emerged (Levin et al., 2010; Graven et al., 2012c). The Northern deficit in $\Delta^{14}C$ has been linked to a growing dominance of fossil fuel emissions in the Northern Hemisphere as air-sea exchange with ^{14}C-depleted ocean water in the Southern Hemisphere weakened with decreasing atmospheric $\Delta^{14}C$ (Levin et al., 2010; Graven et al., 2012c). $\Delta^{14}C$ in background air has exhibited an average trend of about -5 ‰ yr^{-1} since the 1990s (Graven et al., 2012b; Levin et al., 2013) and $\Delta^{14}C$ in background air was 14-20 ‰ in 2015.

The CMIP6 forcing data for $\Delta^{14}C$ are similar to the forcing data used in the ocean carbon cycle model intercomparison OCMIP2 (Fig. 2), with a few notable differences. The zonal bands are defined slightly differently: for CMIP6 we use boundaries of 30°N and 30°S whereas OCMIP2 used 20°N and 20°S. The OCMIP2 forcing data include spatial differences over the period 1955-1968 only, for all other periods the same $\Delta^{14}C$ is used for all three zonal bands. Over the peak $\Delta^{14}C$ period 1962-64 the OCMIP2 forcing data for the tropics are 50-125 ‰ higher than CMIP6, whereas differences for the Northern and Southern Hemispheres are smaller, less than 50 ‰. Larger differences in $\Delta^{14}C$ in the tropics may be partly due to a lack of data in the southern tropics over 1962-64. Measurements by Nydal and Lövseth (1983) in Madagascar (21°S) only started in late 1964 and, compared to their observation sites in the northern tropics, the data from Madagascar show tropical gradients up to 100‰ in 1965.

Two other periods where the CMIP6 forcing data noticeably deviate from the OCMIP2 forcing data are 1976-82, when the OCMIP2 forcing data are 10-30 ‰ higher than the CMIP6 forcing data, and 1992-95, the OCMIP2 forcing data are approx. 10 ‰ lower. For these periods, the OCMIP2 forcing data appears to also be inconsistent with the Hua et al. (2013) compilation (Fig. 2). The OCMIP2 forcing data ends in 1995, but the 1995 value (107 ‰) is also appended for the year 2000 in the OCMIP2 forcing data, which is approx. 15 ‰ higher than the observed $\Delta^{14}C$ in 2000.

4 Historical atmospheric forcing dataset for $\delta^{13}C$ in CO_2

We compiled historical data for $\delta^{13}C$ in atmospheric CO_2 from ice core and firn records and from flask measurements to produce the historical atmospheric forcing dataset. We use the data to estimate annual mean, global mean values for $\delta^{13}C$ (Fig. 1, Fig. 3) as described below. We combine the most extensive dataset for firn and ice core $\delta^{13}C$ measurements for the period after 1850 (Rubino et al., 2013) with recent flask data from three laboratories, including the earliest flask data currently available. This approach provides a consistent data set that incorporates ice core data spanning the historical period and higher temporal resolution in the flask data available starting in 1978-80.

The ice core and firn $\delta^{13}C$ records are from Law Dome and South Pole, comprising 154 individual samples measured by CSIRO (Rubino et al., 2013). Due to the high snow accumulation rate at Law Dome, the firn and ice core record has high time resolution, air age distribution (68% width) of 8 years or less (Rubino et al., 2016), and overlaps the atmospheric record. The datasets published in Rubino et al. (2013) were updated to the latest calibration scale at CSIRO in September 2016. The calibration scale is revised from that presented in Allison &

Francey (2007) with updated corrections for cross contamination effects in the isotope ratio mass spectrometer ion source and ion correction procedures for ^{17}O interference (Brand et al., 2010). The calibration procedure also uses a link to the VPDB reference scale established by the World Meteorological Organization Central Calibration Laboratory (CCL) for stable isotopes in CO_2 (Max Planck Institute for Biogeochemistry, Jena, Germany). The revised procedure ensures that all corrections are consistently applied to all samples measured at CSIRO since 1990, including all ice-core, firn air and flask measurements. We do not include measurements from 24 South Pole firn air samples conducted at NOAA reported in Rubino et al. (2013), because we could not easily quantify any NOAA laboratory offset for these measurements, relative to the current CSIRO calibration.

We use atmospheric $\delta^{13}C$ measured by flask sampling from CSIRO (Allison and Francey, 2007), NOAA (Vaughn et al., 2004) and SIO (Keeling et al., 2001). Observations from SIO between 1977 and 1992 were made in collaboration with the University of Groningen, using the analytical facilities at the University of Groningen for $\delta^{13}C$ measurement. After 1992, the SIO measurements were conducted solely at SIO (Guenther et al., 2001). Observations of $\delta^{13}C$ by CSIRO began at Cape Grim in 1978 and expanded to a global network in the 1980s. CSIRO $\delta^{13}C$ data prior to the early 1990s is not as well calibrated and therefore not publicly available except for Cape Grim, which has data available from the early 1980s. Observations of $\delta^{13}C$ by NOAA and INSTAAR started in the early 1990s. Atmospheric $\delta^{13}C$ data were downloaded in July 2016 from CSIRO, NOAA and SIO. Websites for data access are listed in Table 1.

Here we use atmospheric $\delta^{13}C$ data from two sites, South Pole (SPO) and Mauna Loa (MLO), in order to capture interhemispheric differences in $\delta^{13}C$ in defining a global mean value. These two sites are measured by all three laboratories. In order to compile data from the three laboratories, we used a third station, Alert, Canada, to assess inter-laboratory offsets, also referred to as "scale offsets". There is ongoing work in the community to incorporate best practices for preparing and measuring reference materials, and to use CCL CO_2-in-air reference materials to evaluate and resolve scale offsets in atmospheric $\delta^{13}C$ data (Wendeberg et al., 2013; WMO/IAEA, 2016), however, not all currently reported data consistently account for any scale offsets between laboratories. We adjust SIO and NOAA $\delta^{13}C$ data to be consistent with CSIRO $\delta^{13}C$ data using scale offsets identified in measurements from Alert. Average differences between annual mean $\delta^{13}C$ observations made at Alert for 2005-2015 by CSIRO and by the Max Planck Institute for Biogeochemistry (the CCL) are less than 0.01 ‰ (WMO/IAEA, 2016), so the compiled $\delta^{13}C$ record we present here can also be regarded to be consistent with the VPDB scale established by the CCL.

Comparing annual mean $\delta^{13}C$ observed at Alert over 1992-2014 shows that data reported by NOAA were 0.031 ‰ higher than CSIRO, and data reported by SIO were 0.046 ‰ higher than CSIRO, on average. The standard deviation in NOAA-CSIRO differences was 0.018 ‰, and 0.020 ‰ for SIO-CSIRO differences, with standard error of 0.004 ‰ for both. Similar offsets were found in comparisons of monthly mean rather than annual mean $\delta^{13}C$ at Alert, with larger standard deviations of 0.031 ‰ for monthly NOAA-CSIRO differences and 0.044 ‰ for monthly SIO-CSIRO differences, but smaller standard errors of 0.002 ‰ for both. The offset 0.031 ‰ was subtracted from NOAA data at South Pole and Mauna Loa, and 0.046 ‰ was subtracted from SIO data at South Pole and Mauna Loa. Then the monthly values from the three laboratories were averaged, and used to calculate combined annual means. As a result of varying data availability, annual means for 1977-90 at SPO and 1980-89

at MLO are based only on SIO data (with the offset applied), and the annual mean for 2015 is based only on CSIRO data.

The atmospheric data show a gradient of -0.043 ‰ between Mauna Loa and South Pole in 1980-84, growing to -0.095 ‰ in 2010-14 (Fig 3). Keeling et al. (2011) suggest that the preindustrial Northern Hemisphere – Southern Hemisphere $\delta^{13}C$ gradient was +0.09 ‰, opposite in sign to the present interhemispheric gradient, using a regression of SIO $\delta^{13}C$ data with global total fossil fuel emissions. They further demonstrate that the inferred preindustrial gradient is consistent with a model of spatial variation in equilibrium fractionation during air-sea gas exchange. A similar preindustrial atmospheric $\delta^{13}C$ gradient was simulated by Murnane and Sarmiento (2000) using a global ocean model, where they also attributed the primary driver of the gradient to equilibrium fractionation. $\delta^{13}C$ data from Greenland ice cores and possibly deep firn are compromised by in situ CO_2 production so it is not possible to discern a precise preindustrial or pre-1980 $\delta^{13}C$ gradient directly from observations (Anklin et al., 1995; Francey et al., 1999; Tschumi and Stauffer, 2000; Jenk et al., 2016). We account for the possibility that $\delta^{13}C$ measured in ice core and firn in Antarctica is slightly different from the global mean by using the regression from Keeling et al. (2011) to estimate $\delta^{13}C$ at MLO. Then to estimate global $\delta^{13}C$ we average the observed Antarctic ice core and firn $\delta^{13}C$ and the estimated $\delta^{13}C$ for MLO. Previous studies have adjusted Antarctic ice core and firn $\delta^{13}C$ to estimate global levels by assuming that the preindustrial gradient was zero (Rubino et al., 2013).

To calculate a smoothed, global average time series for $\delta^{13}C$ in CO_2 over 1850-2015, we first average replicate measurements of ice core and firn samples from Rubino et al. (2013) and then calculate annual averages for any year that includes an ice core or firn measurement. Using the annual averages, we estimate a corresponding $\delta^{13}C$ at MLO from the ice core and firn data using the regression from Keeling et al. (2011). We then append the ice core and firn data before 1977 to the annual average record at SPO beginning in 1978, omitting any ice core and firn data after 1978. We similarly append the $\delta^{13}C$ at MLO estimated from the ice core and firn data to the annual average record at MLO beginning in 1980, omitting any ice core and firn- based estimates after 1980 (Fig. 3). Smoothed curves were then calculated for SPO and MLO with stronger weighting on the recent flask-based data to account for the coarser time resolution of the ice core versus flask data due to diffusive smoothing in the firn. Then these curves were averaged and evaluated in the middle of each year 1850-2015 to produce the atmospheric forcing data (Fig 1).

Ice core and firn data after 1977 or 1980 were not used directly to produce the forcing data, but they are included in Fig. 3 for comparison. The differences between SPO annual means and ice core and firn data after 1977 are less than 0.05 ‰ for 14 samples, and less than 0.09 ‰ for the two other samples. The differences between MLO annual means and estimates of MLO $\delta^{13}C$ from ice core and firn data after 1980 are less than 0.03 ‰ for 8 samples, and less than 0.09 ‰ for the one other sample. In addition, applying the regression to the annual mean SPO $\delta^{13}C$ flask data is consistent with MLO observations to within 0.05 ‰, suggesting the regression from Keeling et al. (2011) using 1979-2003 SIO data is also consistent with combined means including the NOAA and CSIRO data, and with the longer period encompassing 2004-2015.

We also compare the global $\delta^{13}C$ forcing data with the global monthly mean Marine Boundary Layer $\delta^{13}C$ estimated from NOAA's larger network of stations, which is available for 1993-2015 (Fig. 3,

www.esrl.noaa.gov/gmd/ccgg/mbl/mbl.html) (Masarie and Tans, 1995). Here the NOAA-CSIRO offset has been applied (0.031 ‰). The differences for 1993-96 are -0.04±0.01 ‰, when the NOAA Marine BL global mean is close to MLO. Differences after 1996 are smaller, -0.02±0.01 ‰. Slightly lower values in NOAA Marine BL global mean indicates low- $\delta^{13}C$ air from the Northern Hemisphere is slightly underrepresented in the MLO-SPO average. However, the long-term trends are similar: both decreased by 0.6 ‰ between 1993 and 2015.

5 Discussion and Conclusions

We have produced a compilation of atmospheric datasets for $\Delta^{14}C$ and $\delta^{13}C$ in CO_2 over the historical period 1850-2015 with the aim of providing a standard atmospheric boundary condition for ocean and terrestrial biosphere models simulating ^{14}C and ^{13}C in CMIP6. The data can be accessed in in Table S1 and at input4MIPs (Graven et al., 2017ab): https://esgf-node.llnl.gov/search/input4mips/.

In compiling these atmospheric forcing datasets for $\Delta^{14}C$ and $\delta^{13}C$ in CO_2, our primary objective was to accurately and consistently compile the data available. We also aimed to provide datasets that are simple to use, particularly as $\delta^{13}C$ has not been included previously in a large model intercomparison. $\Delta^{14}C$ was included previously in OCMIP2 using a similar approach and atmospheric forcing dataset (Orr et al., 1999), but has been updated and improved in this version.

Several applications for simulations of ^{14}C and ^{13}C may require or benefit from the use of oceanic, terrestrial and/or other atmospheric data, including atmospheric data with higher temporal or spatial resolution. Available global-scale databases are listed in Table 1, and we encourage modellers to collaborate with data providers on model-data integration studies. In particular, data users should take care to account for any $\delta^{13}C$ scale offsets between laboratories, as described above. The compilation of various datasets for $\Delta^{14}C$ and $\delta^{13}C$ in CO_2 for modelling and model-data integration studies in the future will benefit from ongoing efforts to compare and harmonize $\Delta^{14}C$ and $\delta^{13}C$ measurements from different laboratories (Miller et al., 2013;Hammer et al., 2016;Wendeberg et al., 2013;WMO/IAEA, 2016), and from additional support for such efforts.

We note that ice core and firn $\delta^{13}C$ data updated from Rubino et al. (2013) that were used to produce the $\delta^{13}C$ forcing data are included in Table S2. The ice core and firn CO_2 data are also included in Table S2. These data could be joined with CSIRO observations at SPO, available from the World Data Centre for Greenhouse Gases (Table 1), to provide Antarctic records of CO_2 concentration and $\delta^{13}C$ measured in the same air sample by the same laboratory, which may be advantageous for some applications.

Data and code availability. The atmospheric forcing datasets for $\Delta^{14}C$ and $\delta^{13}C$ in CO_2 can be accessed in Table S1 and at input4MIPs (Graven et al., 2017ab): https://esgf-node.llnl.gov/search/input4mips/. Original atmospheric data are available from the websites listed in Table 1, and ice core and firn $\delta^{13}C$ data updated from Rubino et al. (2013) are included in Table S2. Interpolation and smoothing were conducted with standard routines in Matlab; further details are available from the lead author on request. A table summarizing the data sources for the $\Delta^{14}C$ compilation is given in Table S3.

Acknowledgments. We thank the staff of the atmospheric monitoring stations for their long-term commitment to the flask sampling activities. The teams of the Law Dome and South Pole drilling expeditions provided the firn air and ice core samples. CSIRO GASLAB and ICELAB personnel supported the measurements of air from the CSIRO monitoring network and firn and ice core samples. Logistic support was provided by the Australian Antarctic Division (Macquarie Island, Law Dome) and the Bureau of Meteorology (Cape Grim, Macquarie Island). The Australian Climate Change Science Program contributed to funding of the CSIRO measurements. Measurements at SIO were supported by the US National Science Foundation, Department of Energy, and NASA under grants 1304270, DE-SC0012167, and NNX17AE74G, by The Eric and Wendy Schmidt Fund for Strategic Innovation, and by NOAA for collection of air samples. Measurements at NOAA and INSTAAR were supported by the NOAA Climate Program Office. Measurements at Heidelberg University were partly funded by a number of agencies in Germany and Europe, namely the Heidelberg Academy of Sciences, the Ministry of Education and Science, Baden-Wurttemberg, Germany; the German Science Foundation, the German Minister of Environment; the German Minister of Science and Technology; the German Umweltbundesamt and the European Commission, Brussels, as well as national funding agencies in Australia, Canada and Spain. H. Graven received support from the European Commission through a Marie Curie Career Integration Grant.

References

Allison, C. E., and Francey, R. J.: Verifying Southern Hemisphere trends in atmospheric carbon dioxide stable isotopes, J Geophys Res, 112, D21304, doi:10.1029/2006jd007345, 2007.

Anklin, M., Barnola, J.-M., Schwander, J., Stauffer, B., and Raynaud, D.: Processes affecting the CO_2 concentrations measured in Greenland ice, Tellus B, 47, 461-470, doi:10.1034/j.1600-0889.47.issue4.6.x, 1995.

Ballantyne, A. P., Miller, J. B., Baker, I. T., Tans, P. P., and White, J. W. C.: Novel applications of carbon isotopes in atmospheric CO_2: what can atmospheric measurements teach us about processes in the biosphere?, Biogeosciences, 8, 3093-3106, doi:10.5194/bg-8-3093-2011, 2011.

Brand, W. A., Assonov, S. S., and Coplen, T. B.: Correction for the ^{17}O interference in $\delta(^{13}C)$ measurements when analyzing CO_2 with stable isotope mass spectrometry (IUPAC Technical Report), pac, 82, 1719-1733, doi:10.1351/pac-rep-09-01-05, 2010.

Braziunas, T. F., Fung, I. Y., and Stuiver, M.: The preindustrial atmospheric $^{14}CO_2$ latitudinal gradient as related to exchanges among atmospheric, oceanic and terrestrial reservoirs, Glob Biogeochem Cycles, 9, 565-584, 1995.

Currie, K. I., Brailsford, G., Nichol, S., Gomez, A., Sparks, R., Lassey, K. R., and Riedel, K.: Tropospheric $^{14}CO_2$ at Wellington, New Zealand: the world's longest record, Biogeochemistry, 104, 5-22, doi:10.1007/s10533-009-9352-6, 2009.

Damon, P. E., Lerman, J. C., and Long, A.: Temporal Fluctuations of Atmospheric ^{14}C: Causal Factors and Implications, Annu Rev Earth Pl Sc, 6, 457-494, 1978.

Fiadeiro, M.: 3-Dimensional Modeling of Tracers in the Deep Pacific-Ocean. 2. Radiocarbon and the Circulation J Mar Res, 40, 537-550, 1982.

Francey, R., Allison, C., Etheridge, D., Trudinger, C., Enting, I., Leuenberger, M., Langenfelds, R., Michel, E., and Steele, L. P.: A 1000-year high precision record of $\delta^{13}C$ in atmospheric CO_2, Tellus B, 51, 170-193, 1999.

Francey, R. J., and Goodman, H. S.: Systematic error in, and selection of Cape Grim in-situ $\delta^{13}C$, in: Baseline Atmospheric Program (Australia) 1983-84 (pp. 27-36), edited by: Francey, R. J., and Forgan, B. W., Department of Science - Bureau of Meteorology and CSIRO - Division of Atmospheric Research, Melbourne, Australia, 1986.

Francey, R. J., Steele, L. P., Langenfelds, R. L., Lucarelli, M., Allison, C. E., Beardsmore, D. J., Coram, S. A., Derek, N., de Silva, F. R., Etheridge, D. M., Fraser, P. J., Henry, R. J., Turner, B., and Welch, E. D.: Global Atmospheric Sampling Laboratory (GASLAB): Supporting and extending the Cape Grim trace gas programs, in: Baseline Atmospheric Program (Australia) 1993 (pp. 8-29), edited by: Francey, R. J., Dick, A. L., and Derek, N., Bureau of Meteorology and CSIRO Division of Atmospheric Research, Melbourne, Australia., 1996.

Graven, H., Allison, C., Etheridge, D., Hammer, S., Keeling, R., Levin, I., Meijer, H. A. J., Rubino, M., Tans, P., Trudinger, C., Vaughn, B., and White, J.: Compiled Historical Record of Atmospheric delta13CO2 version 1.1. Version 20170807, Earth System Grid Federation, doi:10.22033/ESGF/input4MIPs.1601, 2017a.

Graven, H., Allison, C., Etheridge, D., Hammer, S., Keeling, R., Levin, I., Meijer, H. A. J., Rubino, M., Tans, P., Trudinger, C., Vaughn, B., and White, J.: Compiled Historical Record of Atmospheric Delta14CO2 version 2.0. Version 20170807, Earth System Grid Federation, doi:10.22033/ESGF/input4MIPs.1602, 2017b.

Graven, H. D., Gruber, N., Key, R., Khatiwala, S., and Giraud, X.: Changing controls on oceanic radiocarbon: New insights on shallow-to-deep ocean exchange and anthropogenic CO_2 uptake, J Geophys Res, 117, C10005, doi:10.1029/2012JC008074, 2012a.

Graven, H. D., Guilderson, T. P., and Keeling, R. F.: Observations of radiocarbon in CO_2 at La Jolla, California, USA 1992-2007: Analysis of the long-term trend, J Geophys Res, 117, D02302, doi:10.1029/2011JD016533, 2012b.

Graven, H. D., Guilderson, T. P., and Keeling, R. F.: Observations of radiocarbon in CO_2 at seven global sampling sites in the Scripps flask network: Analysis of spatial gradients and seasonal cycles, J Geophys Res, 117, D02303, doi:10.1029/2011JD016535, 2012c.

Graven, H. D.: Impact of fossil fuel emissions on atmospheric radiocarbon and various applications of radiocarbon over this century, P Natl Acad Sci USA, 112, 9542-9545, doi:10.1073/pnas.1504467112, 2015.

Griffies, S. M., Danabasoglu, G., Durack, P. J., Adcroft, A. J., Balaji, V., Böning, C. W., Chassignet, E. P., Curchitser, E., Deshayes, J., Drange, H., Fox-Kemper, B., Gleckler, P. J., Gregory, J. M., Haak, H., Hallberg, R. W., Heimbach, P., Hewitt, H. T., Holland, D. M., Ilyina, T., Jungclaus, J. H., Komuro, Y., Krasting, J. P., Large, W. G., Marsland, S. J., Masina, S., McDougall, T. J., Nurser, A. J. G., Orr, J. C., Pirani, A., Qiao, F., Stouffer, R. J., Taylor, K. E., Treguier, A. M., Tsujino, H., Uotila, P., Valdivieso, M., Wang, Q., Winton, M., and Yeager, S. G.: OMIP contribution to CMIP6: experimental and diagnostic protocol for the physical component of the Ocean Model Intercomparison Project, Geosci Model Dev, 9, 3231-3296, doi:10.5194/gmd-9-3231-2016, 2016.

Guenther, P. R., Bollenbacher, A. F., Keeling, C. D., Stewart, E. F., and Wahlen, M.: Calibration Methodology for the Scripps $^{13}C/^{12}C$ and $^{18}O/^{16}O$ Stable Isotope Program 1969-2000. A Report Prepared for the Global Environmental Monitoring Program of the World Meteorological Organization, Scripps Institution of Oceanography, La Jolla, California, 2001.

Hammer, S., Friedrich, R., Kromer, B., Cherkinsky, A., Lehman, S. J., Meijer, H. A. J., Nakamura, T., Palonen, V., Reimer, R. W., Smith, A. M., Southon, J. R., Szidat, S., Turnbull, J., and Uchida, M.: Compatibility of Atmospheric $^{14}CO_2$ Measurements: Comparing the Heidelberg Low-Level Counting Facility to International Accelerator Mass Spectrometry (AMS) Laboratories, Radiocarbon, 59, 1-9, doi:10.1017/RDC.2016.62, 2016.

Hammer, S., and Levin, I.: Monthly mean atmospheric $\Delta^{14}CO_2$ at Jungfraujoch and Schauinsland from 1986 to 2016, https://heidata.uni-heidelberg.de/dataset.xhtml?persistentId=doi:10.11588/data/10100, doi:10.11588/data/10100, 2017.

He, Y., Trumbore, S. E., Torn, M. S., Harden, J. W., Vaughn, L. J. S., Allison, S. D., and Randerson, J. T.: Radiocarbon constraints imply reduced carbon uptake by soils during the 21st century, Science, 353, 1419-1424, doi:10.1126/science.aad4273, 2016.

Hesshaimer, V., and Levin, I.: Revision of the stratospheric bomb $^{14}CO_2$ inventory, J Geophys Res, 105, 11641-11658, doi:10.1029/1999JD901134, 2000.

Hogg, A. G., Hua, Q., Blackwell, P. G., Niu, M., Buck, C. E., Guilderson, T., Heaton, T. J., Palmer, J. G., Reimer, P. J., Reimer, R. W., Turney, C. S. M., and Zimmerman, S. R. H.: SHCal13 Southern Hemisphere Calibration, 0-50,000 Years Cal BP, Radiocarbon, 55, 1889-1903, doi:10.2458/azu_js_rc.55.16783, 2013.

Hua, Q., Barbetti, M., Zoppi, U., Fink, D., Watanasak, M., and Jacobsen, G. E.: Radiocarbon in tropical tree rings during the Little Ice Age, Nuclear instruments & methods in physics research. Section B, Beam interactions with materials and atoms, 223–224, 489-494, doi:10.1016/j.nimb.2004.04.092, 2004.

Hua, Q., Barbetti, M., and Rakowski, A. Z.: Atmospheric Radiocarbon for the Period 1950–2010, Radiocarbon, 55, 2059–2072, doi:10.2458/azu_js_rc.v55i2.16177, 2013.

IPCC: Climate Change 2013: The Physical Science Basis. Contribution of Working Group I to the Fifth Assessment Report of the Intergovernmental Panel on Climate Change Cambridge University Press, Cambridge, United Kingdom and New York, NY, USA, 1535 pp, 2013.

Jahn, A., Lindsay, K., Giraud, X., Gruber, N., Otto-Bliesner, B. L., Liu, Z., and Brady, E. C.: Carbon isotopes in the ocean model of the Community Earth System Model (CESM1), Geosci Model Dev, 8, 2419-2434, doi:10.5194/gmd-8-2419-2015, 2015.

Jenk, T. M., Rubino, M., Etheridge, D., Ciobanu, V. G., and Blunier, T.: A new set-up for simultaneous high-precision measurements of CO_2, $\delta^{13}C$-CO_2 and $\delta^{18}O$-CO_2 on small ice core samples, Atmos Meas Tech, 9, 3687-3706, doi:10.5194/amt-9-3687-2016, 2016.

Jones, C. D., Arora, V., Friedlingstein, P., Bopp, L., Brovkin, V., Dunne, J., Graven, H., Hoffman, F., Ilyina, T., John, J. G., Jung, M., Kawamiya, M., Koven, C., Pongratz, J., Raddatz, T., Randerson, J. T., and Zaehle, S.:

C4MIP – The Coupled Climate–Carbon Cycle Model Intercomparison Project: experimental protocol for CMIP6, Geosci Model Dev, 9, 2853-2880, doi:10.5194/gmd-9-2853-2016, 2016.
Joos, F., Bruno, M., Fink, R., Siegenthaler, U., Stocker, T. F., Le Quéré, C., and Sarmiento, J. L.: An efficient and accurate representation of complex oceanic and biospheric models of anthropogenic carbon uptake, Tellus B, 48, 397-417, doi:10.3402/tellusb.v48i3.15921, 1996.
Karlen, I., Olsson, I. U., Kallburg, P., and Kilici, S.: Absolute determination of the activity of two ^{14}C dating standards, Arkiv Geofysik, 4, 465-471, 1965.
Keeling, C. D.: The Suess effect: ^{13}Carbon-^{14}Carbon interrelations, Environment Int, 2, 229-300, doi:10.1016/0160-4120(79)90005-9, 1979.
Keeling, C. D., Mook, W. G., and Tans, P. P.: Recent trends in the $^{13}C/^{12}C$ ratio of atmospheric carbon dioxide, Nature, 277, 121-123, 1979.
Keeling, C. D., Piper, S. C., Bacastow, R. B., Wahlen, M., Whorf, T. P., Heimann, M., and Meijer, H. A.: Exchanges of atmospheric CO_2 and $^{13}CO_2$ with the terrestrial biosphere and oceans from 1978 to 2000. I. Global aspects. SIO REFERENCE NO. 01-06, Scripps Institution of Oceanography, La Jolla, California, 2001.
Keeling, C. D., Piper, S. C., Bacastow, R. B., Wahlen, M., Whorf, T. P., Heimann, M., and Meijer, H. A.: Atmospheric CO_2 and $^{13}CO_2$ exchange with the terrestrial biosphere and oceans from 1978 to 2000: observations and carbon cycle implications, A History of Atmospheric CO_2 and its effects on Plants, Animals, and Ecosystems, edited by: Ehleringer, J. R., Cerling, T. E., and Dearing, M. D., Springer Verlag, New York, 2005.
Keeling, C. D., Piper, S. C., Whorf, T. P., and Keeling, R. F.: Evolution of natural and anthropogenic fluxes of atmospheric CO_2 from 1957 to 2003, Tellus B, 63, 1-22, doi:10.1111/j.1600-0889.2010.00507.x, 2011.
Keeling, R. F., Graven, H. D., Welp, L. R., Resplandy, L., Bi, J., Piper, S. C., Sun, Y., Bollenbacher, A., and Meijer, H. A. J.: Atmospheric evidence for a global secular increase in carbon isotopic discrimination of land photosynthesis, Proceedings of the National Academy of Sciences, 114, 10361-10366, 10.1073/pnas.1619240114, 2017.
Keller, K. M., Lienert, S., Bozbiyik, A., Stocker, T. F., Churakova, O. V., Frank, D. C., Klesse, S., Koven, C. D., Leuenberger, M., Riley, W. J., Saurer, M., Siegwolf, R., Weigt, R. B., and Joos, F.: 20th century changes in carbon isotopes and water-use efficiency: tree-ring-based evaluation of the CLM4.5 and LPX-Bern models, Biogeosciences, 14, 2641-2673, doi:10.5194/bg-14-2641-2017, 2017.
Key, R. M., Kozyr, A., Sabine, C. L., Lee, K., Wanninkhof, R., Bullister, J. L., Feely, R. A., Millero, F. J., Mordy, C., and Peng, T. H.: A global ocean carbon climatology: Results from Global Data Analysis Project (GLODAP), Glob Biogeochem Cycles, 18, GB4031, 2004.
Khatiwala, S., Primeau, F., and Hall, T.: Reconstruction of the history of anthropogenic CO_2 concentrations in the ocean, Nature, 462, 346-349, doi:10.1038/nature08526, 2009.
Lehman, S. J., Miller, J. B., Wolak, C., Southon, J., Tans, P. P., Montzka, S. A., Sweeney, C., Andrews, A., LaFranchi, B., Guilderson, T. P., and Turnbull, J. C.: Allocation of Terrestrial Carbon Sources Using $^{14}CO_2$: Methods, Measurement, and Modeling, Radiocarbon, 55, 1484-1495, doi:10.1017/S0033822200048414, 2016.
Lerman, J., Mook, W., and Vogel, J.: C14 in tree rings from different localities, Radiocarbon Variations and Absolute Chronology. Proceedings, XII Nobel Symposium. New York: Wiley. p, 1970, 275-301,
Levin, I., Kromer, B., Schoch-Fischer, H., Bruns, M., Munnich, K. O., Berdau, D., Vogel, J. C., and Munnich, K. O.: 25 years of tropospheric ^{14}C observations in Central Europe, Radiocarbon, 27, 1-19, 1985.
Levin, I., Kromer, B., Wagenbach, D., and Munnich, K. O.: Carbon isotope measurements of atmospheric CO_2 at a coastal station in Antarctica, Tellus B, 39B, 89-95, doi:10.1111/j.1600-0889.1987.tb00273.x, 1987.
Levin, I., and Hesshaimer, V.: Radiocarbon – A Unique Tracer of Global Carbon Cycle Dynamics, Radiocarbon, 42, 69-80, 2000.
Levin, I., Naegler, T., Kromer, B., Diehl, M., Francey, R. J., Gomez-Pelaez, A. J., Steele, L. P., Wagenbach, D., Weller, R., and Worthy, D. E.: Observations and modelling of the global distribution and long-term trend of atmospheric $^{14}CO_2$, Tellus B, 62, 26-46, 2010.
Levin, I., Kromer, B., and Hammer, S.: Atmospheric $\Delta^{14}CO_2$ trend in Western European background air from 2000 to 2012, Tellus B, 65, 20092, 2013.
Manning, M. R., Lowe, D. C., Melhuish, W. H., Sparks, R. J., Wallace, G., Brenninkmeijer, C. A. M., and McGill, R. C.: The Use of Radiocarbon Measurements in Atmospheric Studies, Radiocarbon, 32, 37-58, 1990.
Masarie, K. A., and Tans, P. P.: Extension and integration of atmospheric carbon dioxide data into a globally consistent measurement record, J Geophys Res, 100, 11593-11610, doi:10.1029/95JD00859, 1995.
Matsumoto, K., Sarmiento, J. L., Key, R. M., Aumont, O., Bullister, J. L., Caldeira, K., Campin, J. M., Doney, S., Drange, H., Dutay, J. C., Follows, M., Gao, Y., Gnanadesikan, A., Gruber, N., Ishida, A., Joos, F., Lindsay, K., Maier-Reimer, E., Marshall, J. C., Matear, R., Monfray, P., Mouchet, A., Najjar, R., Plattner, G. K., Schlitzer, R., Slater, R., Swathi, P. S., Totterdell, I., Weirig, M. F., Yamanaka, Y., Yool, A., and Orr, J. C.: Evaluation of ocean carbon cycle models with data-based metrics, Geophys Res Lett, 31, L07303, doi:10.1029/2003gl018970, 2004.

McCormac, F. G., Hogg, A. G., Higham, T. F. G., Lynch-Stieglitz, J., Broecker, W. S., Baillie, M. G. L., Palmer, J., Xiong, L., Pilcher, J. R., Brown, D., and Hoper, S. T.: Temporal variation in the interhemispheric ^{14}C offset, Geophys Res Lett, 25, 1321-1324, doi:10.1029/98GL01065, 1998.

Meijer, H., Pertuisot, M., and Van Der Plicht, J.: High-accuracy ^{14}C measurements for atmospheric CO_2 samples by AMS, Radiocarbon, 48, 355-372, 2006.

Meinshausen, M., Vogel, E., Nauels, A., Lorbacher, K., Meinshausen, N., Etheridge, D. M., Fraser, P. J., Montzka, S. A., Rayner, P. J., Trudinger, C. M., Krummel, P. B., Beyerle, U., Canadell, J. G., Daniel, J. S., Enting, I. G., Law, R. M., Lunder, C. R., O'Doherty, S., Prinn, R. G., Reimann, S., Rubino, M., Velders, G. J. M., Vollmer, M. K., Wang, R. H. J., and Weiss, R.: Historical greenhouse gas concentrations for climate modelling (CMIP6), Geosci Model Dev, 10, 2057-2116, doi:10.5194/gmd-10-2057-2017, 2017.

Miller, J., Lehman, S., Wolak, C., Turnbull, J. C., Dunn, G., Graven, H., Keeling, R., Meijer, H. A. J., Aerts-Bijma, A. T., Palstra, S. W. L., Smith, A. M., Allison, C., Southon, J., Xu, X., Nakazawa, T., Aoki, S., Nakamura, T., Guilderson, T., LaFranchi, B., Mukai, H., Terao, Y., Uchida, M., and Kondo, M.: Initial Results of an Intercomparison of AMS-Based Atmospheric $^{14}CO_2$ Measurements, Radiocarbon, 55, 1475-1483, 2013.

Münnich, K. O., and Vogel, J. C.: Durch Atomexplosionen erzeugter Radiokohlenstoff in der Atmosphäre, Die Naturwissenschaften, 45, 327-329, doi:10.1007/BF00640209, 1958.

Murnane, R. J., and Sarmiento, J. L.: Roles of biology and gas exchange in determining the $\delta^{13}C$ distribution in the ocean and the preindustrial gradient in atmospheric $\delta^{13}C$, Glob Biogeochem Cycles, 14, 389-405, doi:10.1029/1998GB001071, 2000.

Naegler, T., and Levin, I.: Closing the global radiocarbon budget 1945–2005, J Geophys Res, 111, D12311, doi:10.1029/2005jd006758, 2006.

Naegler, T.: Reconciliation of excess ^{14}C-constrained global CO_2 piston velocity estimates, Tellus B, 61, 372-384, doi:10.1111/j.1600-0889.2008.00408.x, 2009.

Naegler, T., and Levin, I.: Biosphere-atmosphere gross carbon exchange flux and the $\delta^{13}CO_2$ and $\Delta^{14}CO_2$ disequilibria constrained by the biospheric excess radiocarbon inventory, J Geophys Res, 114, D17303, doi:10.1029/2008jd011116, 2009.

Nydal, R., and Lövseth, K.: Tracing Bomb ^{14}C in the Atmosphere, J Geophys Res, 88, 3621-3642, 1983.

O'Neill, B. C., Tebaldi, C., van Vuuren, D. P., Eyring, V., Friedlingstein, P., Hurtt, G., Knutti, R., Kriegler, E., Lamarque, J. F., Lowe, J., Meehl, G. A., Moss, R., Riahi, K., and Sanderson, B. M.: The Scenario Model Intercomparison Project (ScenarioMIP) for CMIP6, Geosci Model Dev, 9, 3461-3482, doi:10.5194/gmd-9-3461-2016, 2016.

Oeschger, H., Siegenthaler, U., Schotterer, U., and Gugelmann, A.: A box diffusion model to study the carbon dioxide exchange in nature, Tellus, 27, 168-192, 1975.

Orr, J. C., Najjar, R., Sabine, C. L., and Joos, F.: Abiotic-HOWTO. Internal OCMIP Report, Lab. des Sci. du Clim. et l'Environ., 25pp, Gif-sur-Yvette, France, 25 pp., 1999.

Orr, J. C., Maier-Reimer, E., Mikolajewicz, U., Monfray, P., Sarmiento, J. L., Toggweiler, J. R., Taylor, N. K., Palmer, J., Gruber, N., Sabine, C. L., Le Quéré, C., Key, R. M., and Boutin, J.: Estimates of anthropogenic carbon uptake from four three-dimensional global ocean models, Glob Biogeochem Cycles, 15, 43-60, doi:10.1029/2000GB001273, 2001.

Orr, J. C., Najjar, R. G., Aumont, O., Bopp, L., Bullister, J. L., Danabasoglu, G., Doney, S. C., Dunne, J. P., Dutay, J. C., Graven, H., Griffies, S. M., John, J. G., Joos, F., Levin, I., Lindsay, K., Matear, R. J., McKinley, G. A., Mouchet, A., Oschlies, A., Romanou, A., Schlitzer, R., Tagliabue, A., Tanhua, T., and Yool, A.: Biogeochemical protocols and diagnostics for the CMIP6 Ocean Model Intercomparison Project (OMIP), Geosci Model Dev, 10, 2169-2199, doi:10.5194/gmd-10-2169-2017, 2017.

Quay, P., Sonnerup, R., Westby, T., Stutsman, J., and McNichol, A.: Changes in the $^{13}C/^{12}C$ of dissolved inorganic carbon in the ocean as a tracer of anthropogenic CO_2 uptake, Glob Biogeochem Cycles, 17, 1004, doi:10.1029/2001gb001817, 2003.

Rafter, T. A., and Fergusson, G. J.: "Atom Bomb Effect"--Recent Increase of Carbon-14 Content of the Atmosphere and Biosphere, Science, 126, 557-558, 1957.

Randerson, J. T., Collatz, G. J., Fessenden, J. E., Munoz, A. D., Still, C. J., Berry, J. A., Fung, I. Y., Suits, N., and Denning, A. S.: A possible global covariance between terrestrial gross primary production and ^{13}C discrimination: Consequences for the atmospheric ^{13}C budget and its response to ENSO, Glob Biogeochem Cycles, 16, 1136, doi:10.1029/2001gb001845, 2002.

Reimer, P. J., Bard, E., Bayliss, A., Beck, J. W., Blackwell, P. G., Bronk Ramsey, C., Buck, C. E., Cheng, H., Edwards, R. L., Friedrich, M., Grootes, P., Guilderson, T., Haflidason, H., Hajdas, I., Hatte, C., Heaton, T. J., Hoffmann, D. L., Hogg, A. G., Hughen, K. A., Kaiser, K. F., Kromer, B., Manning, S. W., Niu, M., Reimer, R. W., Richards, D. A., Scott, E. M., Southon, J. R., Staff, R. A., Turney, C. S. M., and van Der Plicht, J.: IntCal13 and Marine13 radiocarbon age calibration curves 0–50,000 years cal BP, Radiocarbon, 55, 1869–1887, doi:10.2458/azu_js_rc.55.16947, 2013.

Revelle, R., and Suess, H. E.: Carbon Dioxide Exchange Between Atmosphere and Ocean and the Question of an Increase of Atmospheric CO_2 during the Past Decades, Tellus, 9, 18-27, doi:10.1111/j.2153-3490.1957.tb01849.x, 1957.

Rodgers, K. B., Mikaloff-Fletcher, S. E., Bianchi, D., Beaulieu, C., Galbraith, E. D., Gnanadesikan, A., Hogg, A. G., Iudicone, D., Lintner, B. R., Naegler, T., Reimer, P. J., Sarmiento, J. L., and Slater, R. D.: Interhemispheric gradient of atmospheric radiocarbon reveals natural variability of Southern Ocean winds, Clim Past, 7, 1123-1138, doi:10.5194/cp-7-1123-2011, 2011.

Rubino, M., Etheridge, D. M., Trudinger, C. M., Allison, C. E., Battle, M. O., Langenfelds, R. L., Steele, L. P., Curran, M., Bender, M., White, J. W. C., Jenk, T. M., Blunier, T., and Francey, R. J.: A revised 1000 year atmospheric $\delta^{13}C$-CO_2 record from Law Dome and South Pole, Antarctica, J Geophys Res Atmos, 118, 8482-8499, doi:10.1002/jgrd.50668, 2013.

Rubino, M., Etheridge, D. M., Trudinger, C. M., Allison, C. E., Rayner, P. J., Enting, I., Mulvaney, R., Steele, L. P., Langenfelds, R. L., Sturges, W. T., Curran, M. A. J., and Smith, A. M.: Low atmospheric CO_2 levels during the Little Ice Age due to cooling-induced terrestrial uptake, Nature Geosci, 9, 691-694, doi:10.1038/ngeo2769, 2016.

Santos, G. M., Linares, R., Lisi, C. S., and Tomazello Filho, M.: Annual growth rings in a sample of Paraná pine (Araucaria angustifolia): Toward improving the ^{14}C calibration curve for the Southern Hemisphere, Quaternary Geochronology, 25, 96-103, doi:10.1016/j.quageo.2014.10.004, 2015.

Schmittner, A., Gruber, N., Mix, A. C., Key, R. M., Tagliabue, A., and Westberry, T. K.: Biology and air-sea gas exchange controls on the distribution of carbon isotope ratios ($\delta^{13}C$) in the ocean, Biogeosciences, 10, 5793-5816, doi:10.5194/bg-10-5793-2013, 2013.

Scholze, M., Ciais, P., and Heimann, M.: Modeling terrestrial ^{13}C cycling: Climate, land use and fire, Glob Biogeochem Cycles, 22, GB1009, doi:10.1029/2006gb002899, 2008.

Stuiver, M., and Polach, H. A.: Discussion: Reporting of ^{14}C Data, Radiocarbon, 19, 355-363, 1977.

Stuiver, M., and Quay, P. D.: Atmospheric ^{14}C changes resulting from fossil fuel CO_2 release and cosmic ray flux variability, Earth Planet Sci Lett, 53, 349-362, 1981.

Suess, H. E.: Radiocarbon concentration in modern wood, Science, 122, 415-417, 1955.

Sweeney, C., Gloor, E., Jacobson, A. R., Key, R. M., McKinley, G., Sarmiento, J. L., and Wanninkhof, R.: Constraining global air-sea gas exchange for CO_2 with recent bomb ^{14}C measurements, Glob Biogeochem Cycles, 21, GB2015, doi:10.1029/2006gb002784, 2007.

Tagliabue, A., and Bopp, L.: Towards understanding global variability in ocean carbon-13, Glob Biogeochem Cycles, 22, GB1025, doi:10.1029/2007GB003037, 2008.

Tans, P. P.: A Compilation of Bomb ^{14}C Data for Use in Global Carbon Model Calculations, in: SCOPE 16 Carbon Cycle Modelling. , edited by: Bolin, B., John Wiley & Sons, 1981.

Thompson, M. V., and Randerson, J. T.: Impulse response functions of terrestrial carbon cycle models: method and application, Glob Chang Biol, 5, 371-394, doi:10.1046/j.1365-2486.1999.00235.x, 1999.

Trumbore, S. E.: Age of Soil Organic Matter and Soil Respiration: Radiocarbon Constraints on Belowground C Dynamics, Ecol Appl, 10, 399-411, 2000.

Tschumi, J., and Stauffer, B.: Reconstructing past atmospheric CO_2 concentration based on ice-core analyses: open questions due to in situ production of CO_2 in the ice, J Glaciol, 46, 45-53, doi:10.3189/172756500781833359, 2000.

Turnbull, J. C., Lehman, S. J., Miller, J. B., Sparks, R. J., Southon, J. R., and Tans, P. P.: A new high precision $^{14}CO_2$ time series for North American continental air, J Geophys Res, 112, D11310, doi:10.1029/2006jd008184, 2007.

Turnbull, J. C., Mikaloff Fletcher, S. E., Ansell, I., Brailsford, G., Moss, R., Norris, M., and Steinkamp, K.: Sixty years of radiocarbon dioxide measurements at Wellington, New Zealand 1954 – 2014, Atmos Chem Phys Discuss, 2016, 1-28, doi:10.5194/acp-2016-1110, 2016.

Vaughn, B. H., Miller, J., Ferretti, D. F., and White, J. W. C.: Chapter 14 - Stable isotope measurements of atmospheric CO_2 and CH_4 in: Handbook of Stable Isotope Analytical Techniques, edited by: de Groot, P. A., Elsevier, p272-304, Amsterdam, 272-304, 2004.

Vaughn, B. H., Evans, C. U., White, J. W. C., Still, C. J., Masarie, K. A., and Turnbull, J.: Global Network Measurements of Atmospheric Trace Gas Isotopes, in: Isoscapes: Understanding Movement, Pattern, and Process on Earth Through Isotope Mapping, edited by: West, J. B., Bowen, G. J., Dawson, T. E., and Tu, K. P., Springer Amsterdam, Netherlands, 3-31, 2010.

Wendeberg, M., Richter, J. M., Rothe, M., and Brand, W. A.: Jena Reference Air Set (JRAS): a multi-point scale anchor for isotope measurements of CO_2 in air, Atmos Meas Tech, 6, 817-822, doi:10.5194/amt-6-817-2013, 2013.

WMO/IAEA: 18th WMO/IAEA Meeting on Carbon Dioxide, Other Greenhouse Gases and Related Tracers Measurement Techniques (GGMT-2015), World Meteorological Organization, Global Atmosphere Watch, 2016.

Table 1. Available global-scale databases of $\Delta^{14}C$ and $\delta^{13}C$ in atmospheric CO_2, terrestrial and ocean carbon, and fossil fuel emissions.

Name	Type	Website
Scripps Institution of Oceanography Global CO_2 Program	$\Delta^{14}C$ and $\delta^{13}C$ in CO_2	http://scrippsco2.ucsd.edu
NOAA Global Greenhouse Gas Reference Network	$\Delta^{14}C$ and $\delta^{13}C$ in CO_2	https://www.esrl.noaa.gov/gmd/dv/data/
World Data Centre for Greenhouse Gases (Including CSIRO data)	$\Delta^{14}C$ and $\delta^{13}C$ in CO_2	http://ds.data.jma.go.jp/gmd/wdcgg/
Heidelberg University data center	$\Delta^{14}C$ in CO_2	https://heidata.uni-heidelberg.de/dataverse/carbon
Carbon Dioxide Information Analysis Center (CDIAC)	$\Delta^{14}C$ and $\delta^{13}C$ in CO_2, and $\delta^{13}C$ in fossil fuel CO_2 emissions	http://cdiac.ess-dive.lbl.gov/
GLobal Ocean Data Analysis Project GLODAP v2	$\Delta^{14}C$ and $\delta^{13}C$ in ocean dissolved inorganic carbon	https://www.nodc.noaa.gov/ocads/oceans/GLODAPv2/
TRY Plant Trait Database	$\delta^{13}C$ in terrestrial plants	https://www.try-db.org/TryWeb/Home.php
International Tree-Ring Data Bank	$\delta^{13}C$ in terrestrial plants	https://www.ncdc.noaa.gov/data-access/paleoclimatology-data/datasets/tree-ring
Soil Carbon Database	$\Delta^{14}C$ and $\delta^{13}C$ in soil carbon	https://github.com/powellcenter-soilcarbon

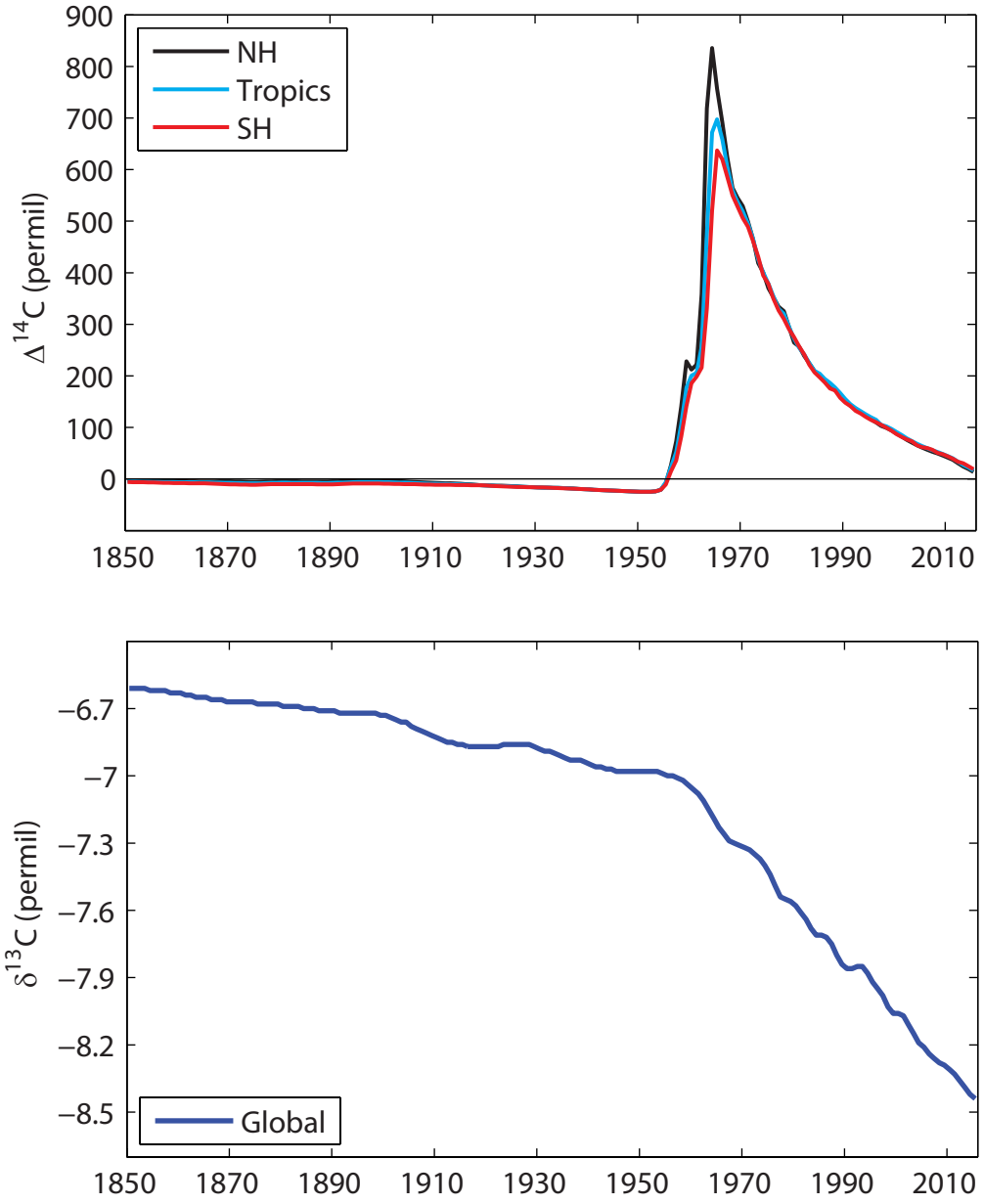

Figure 1. Historical atmospheric forcing datasets for $\Delta^{14}C$ in CO_2 (top) and $\delta^{13}C$ in CO_2 (bottom) compiled for CMIP6. Annual mean values of $\Delta^{14}C$ are provided for three zonal bands representing the Northern Hemisphere (30°N-90°N), the Tropics (30°S-30°N) and the Southern Hemisphere (30°S-90°S). Annual mean, global mean values are provided for $\delta^{13}C$. Tabulated data are provided in Table S1.

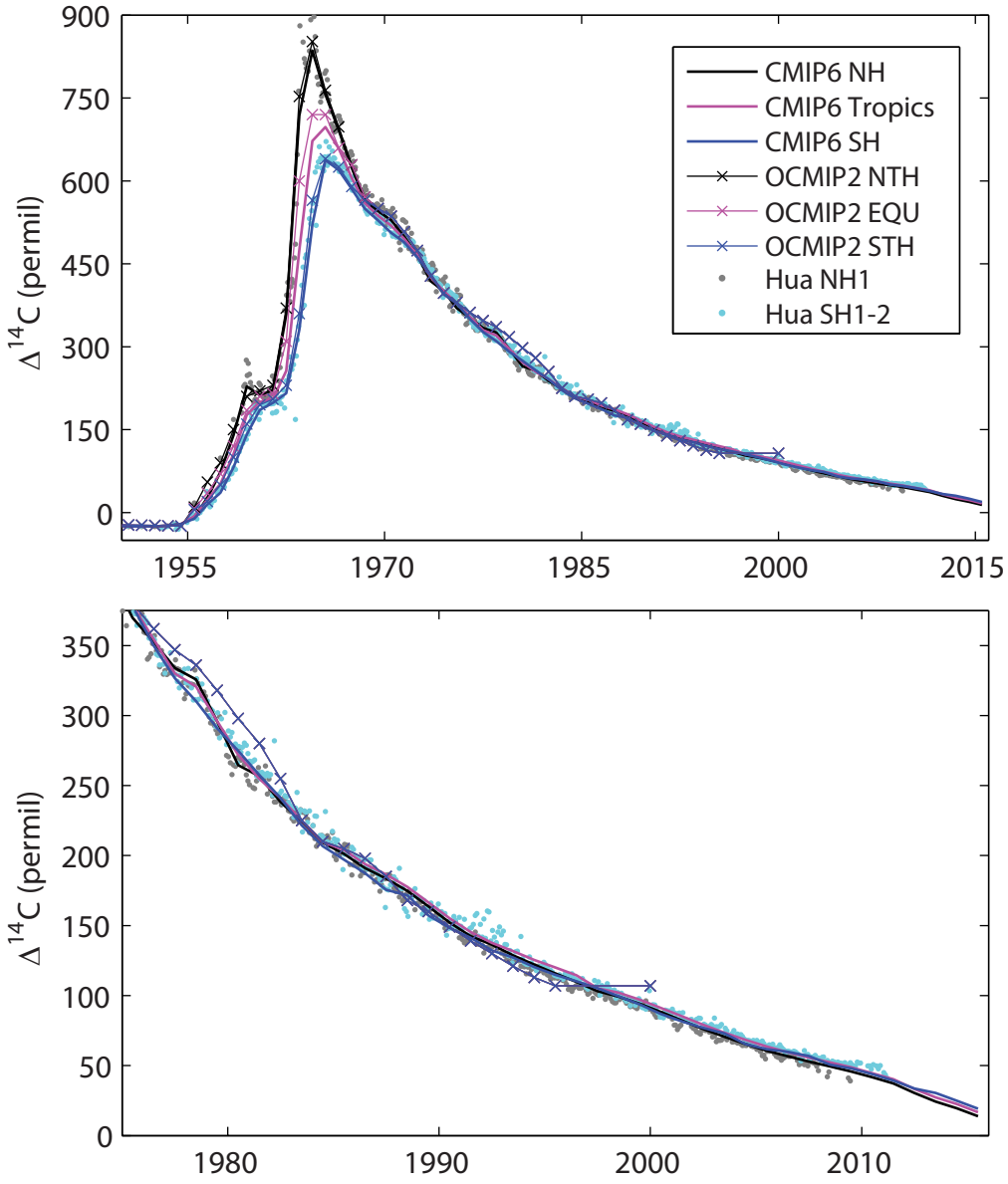

Figure 2. The $\Delta^{14}C$ atmospheric forcing data for CMIP6 compared to the forcing data used in OCMIP2 and the Northern and Southern Hemisphere tree ring and atmospheric data compilations of Hua et al. (2013) over the time period 1950-2015 (top) and over the recent period 1975-2015 (bottom). Zones NH1 and SH1-2 from Hua et al. (2013) are used, to correspond to the Northern Hemisphere north of 30°N and the Southern Hemisphere south of 30°S. Tropical data from Hua et al. (2013) are not shown, for clarity.

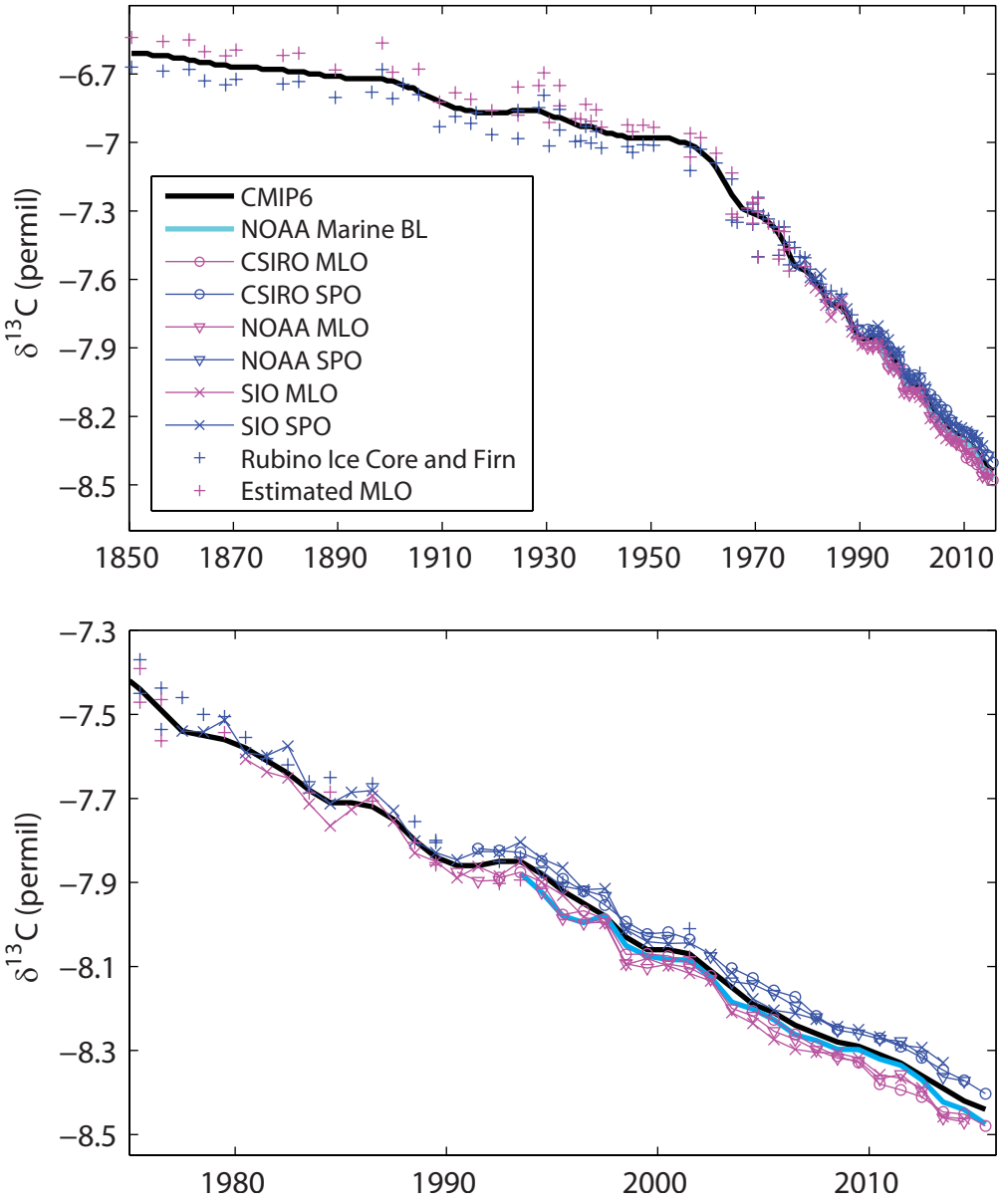

Figure 3. Observations of $\delta^{13}C$ and the $\delta^{13}C$ atmospheric forcing data for CMIP6 over the full time period 1850-2015 (top) and over the recent period 1975-2015 (bottom). The $\delta^{13}C$ atmospheric forcing data for CMIP6 are shown in black, as in Fig. 1. Data from SPO and ice core and firn samples are shown in blue, and data from MLO and estimated data for MLO based on ice core and firn samples and the regression from Keeling et al. (2011) are shown in purple. Measurements conducted at different laboratories are shown with different symbols. Data from NOAA and SIO have been adjusted with their average laboratory offset from CSIRO. The global mean $\delta^{13}C$ estimated by NOAA based on a larger network of flask sampling stations over 1993-2015 is shown in light blue (NOAA Marine Boundary Layer).